Cellular glutathione levels in HL-60 cells during respiratory burst are not correlated with ultra-weak photon emission

Rossetto Burgos, R.C.; Zhang, W.; Wijk, E.P.A. van.; Hankemeier, T.; Ramautar, R.; Greef, J. van der

Journal of Photochemistry & Photobiology, B: Biology 175 (2017) 291–296

Contents lists available at ScienceDirect

Journal of Photochemistry & Photobiology, B: Biology

journal homepage: www.elsevier.com/locate/jphotobiol

Cellular glutathione levels in HL-60 cells during respiratory burst are not correlated with ultra-weak photon emission

Rosilene Cristina Rossetto Burgos[a,b,*], Wei Zhang[a], Eduard P.A. van Wijk[b], Thomas Hankemeier[a], Rawi Ramautar[a], Jan van der Greef[a,b]

[a] Division of Analytical Biosciences, Leiden Academic Centre for Drug Research, Leiden University, P.O. Box 9502, 2300 RA Leiden, The Netherlands
[b] Sino-Dutch Centre for Preventive and Personalized Medicine/Centre for Photonics of Living Systems, Leiden University, P.O. Box 9502, 2300 RA Leiden, The Netherlands

ARTICLE INFO

Keywords:
Ultra-weak photon emission, capillary electrophoresis-mass spectrometry
Glutathione
N-ethylmaleimide
HL-60 cell line
Respiratory burst

ABSTRACT

Recently, ultra-weak photon emission (UPE) was developed as a novel tool for measuring oxidative metabolic processes, as its generation is related to reactive oxygen species (ROS). Both an imbalance in ROS or the uncontrolled production of ROS can lead to oxidative stress, which is commonly associated with many diseases. In addition to playing several biological functions, the thiol amino acid glutathione has an important antioxidant function in the body's defense against ROS. Specifically, glutathione is an important endogenous antioxidant that helps maintain oxidant levels. At the cellular level, glutathione is present in its reduced form (GSH) at relatively high concentrations (in the millimolar range) and in its oxidized form (GSSG) at low concentrations (in the micromolar range). Thus, the GSH/GSSG ratio is often used as an indicator of cellular redox state. Here, we used the HL-60 cell line as a model system in order to determine whether UPE is correlated with intracellular GSH and GSSG levels. HL-60 cells were differentiated into neutrophil-like cells and then stimulated to undergo respiratory burst. We then recorded UPE in real time for 9000 seconds and used capillary electrophoresis coupled to mass spectrometry to measure GSH and GSSG levels in cell extracts. We found that although respiratory burst significantly decreased the GSH/GSSG ratio, this change was not significantly correlated with the UPE profile.

1. Introduction

Ultra-weak photon emission (UPE) is endogenous light emitted by virtually all living systems during oxidative metabolism and under stress conditions [1,2]. During biochemical oxidative reactions, reactive oxygen species (ROS) are generated, leading to the spontaneous emission of weak photons as a result of the electrons' transition from an excited state to the ground state [1,2]. When ROS are produced at high levels, they can react with biomolecules, leading to several forms of damage at the cellular to macromolecular levels; this condition — known as oxidative stress — has been associated with many pathological mechanisms [3–6]. In recent years, UPE has often been associated with oxidative stress based on the notion that UPE is directly linked to ROS production; therefore, UPE has been used as a label-free, non-invasive tool to dynamically monitor oxidative stress during metabolic processes [7]. For example, reactions between radicals and biomolecules such as proteins and lipids (e.g., lipid peroxidation) have been reported to increase UPE intensity [7–9].

Glutathione (L-γ-glutamyl-L-cysteinylglycine, or GSH) is the most abundant thiol amino acid and is present in virtually every cell in the body [10,11]. The biosynthesis of GSH (see Fig. 1) begins with cysteine, glutamate, and glycine and requires two ATP molecules and two enzymatic steps involving γ-glutamylcysteine synthetase and glutathione synthetase [12]. GSH has many biological functions, including the synthesis of proteins and DNA, molecular transport, and redox signaling. However, its function as an antioxidant is the most biologically significant; specifically, GSH functions as a major scavenger of free radicals and ROS [10–12]. Under oxidative conditions, GSH is oxidized via the glutathione peroxidase system to produce glutathione disulfide (GSSG), which can be converted back to GSH via the glutathione reductase system (Fig. 1); this process maintains physiological levels of ROS [10–12]. In this context, glutathione plays a role in the cellular redox system, and the GSH/GSSG ratio has been considered an important indicator of cellular redox state [13]. Because glutathione plays a role in the cellular antioxidant system, UPE may be correlated with the cell's glutathione antioxidant capacity.

As a follow-up to our previous studies [7,14], we examined whether UPE is associated with GSH/GSSG ratio in HL-60 cells during respiratory burst. Given that the GSH/GSSG ratio is often reported as a marker of oxidative stress, our aim was to determine whether UPE

* Corresponding author at: Division of Analytical Biosciences, Leiden Academic Centre for Drug Research, Leiden University, P.O. Box 9502, 2300 RA Leiden, The Netherlands.
E-mail address: r.c.rossetto.burgos@lacdr.leidenuniv.nl (R.C.R. Burgos).

http://dx.doi.org/10.1016/j.jphotobiol.2017.09.002
Received 18 July 2017; Received in revised form 30 August 2017; Accepted 1 September 2017
Available online 07 September 2017

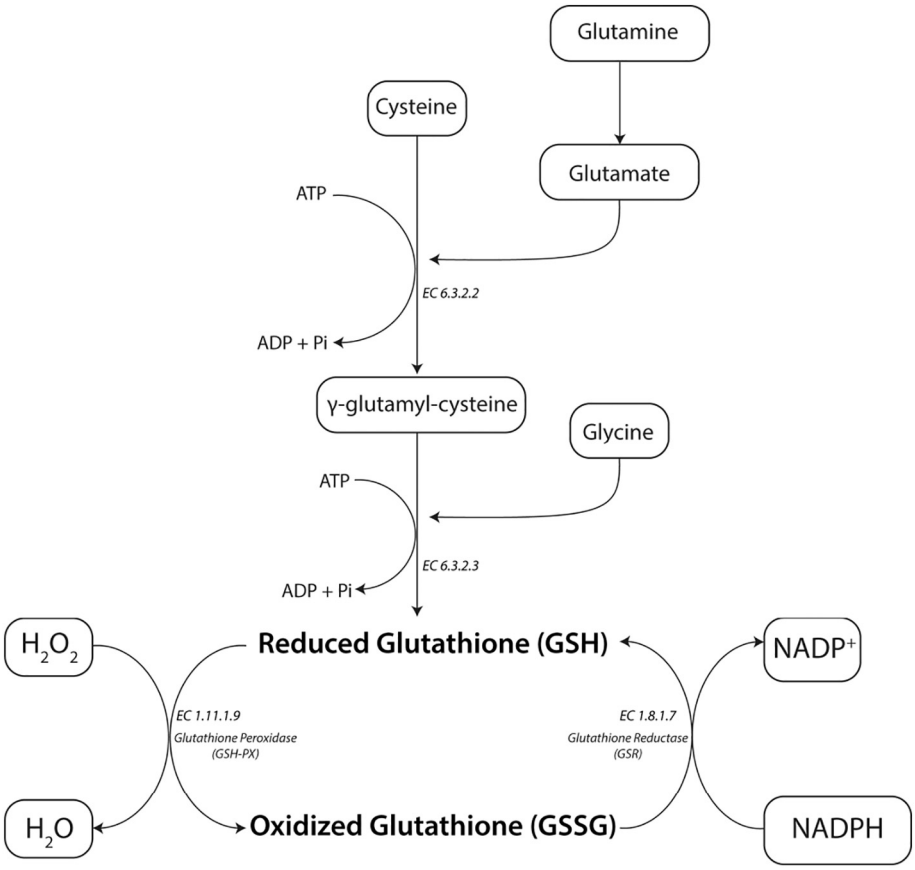

Fig. 1. The biosynthetic pathway for the production, consumption, and regeneration of GSH in biological systems. In the presence of energy (ATP) and γ-glutamylcysteine synthetase (EC 1.8.1.7), cysteine and glutamate are used to produce γ-glutamyl-cysteine. GSH is then formed using a second molecule of ATP and glutathione synthetase (EC 6.3.2.3). In presence of radicals, GSH is oxidized to GSSG via glutathione peroxidase (EC 1.11.1.9). GSSG can then be reduced back to GSH by glutathione reductase (EC 1.8.1.7) using NADPH.

indeed reflects this process and whether UPE can be used as a non-invasive tool for monitoring cellular levels of oxidative stress.

Several methods have been used by various groups to measure GSH and GSSG. Classic approaches such as spectrophotometric-based methods are well described in the literature; the most common of these methods are the glutathione S-transferase 1-chloro-2,4-dinitrobenzene (CDNB) endpoint method and the GSH–5,5′-dithio-bis (2-nitrobenzoic acid) "enzymatic recycling assay" [15–17]. Despite its popularity, however, the CDNB endpoint method measures only GSH and lacks sensitivity [15]; moreover, in both methods GSH can be readily oxidized during sample preparation, leading to an error when calculating GSH and GSSG levels [18,19]. Thus, these methods provide unsatisfactory levels of specificity and selectivity. Chromatographic methods such as HPLC-UV, HPLC-FL, LC-MS, and GC–MS are commonly used to measure glutathione [20,21]. Capillary electrophoresis coupled to mass spectrometry (CE-MS) is particularly well suited due to its high separation efficiency, high selectivity, and low solvent and sample consumption [22,23].

With respect to the auto-oxidation of GSH, several derivatization compounds have been used recently to prevent the oxidation of GSH during sample collection, preparation, and analysis [24,25]. *N*-ethylmaleimide (NEM) is a preferred alkylating agent for the derivatization of GSH for several reasons. First, NEM is a specific alkylating agent for sulfhydryl groups. Second, NEM forms a stable thioether bond by reacting with sulfhydryl groups, leading to the formation of the GSH adducts *N*-ethyl succinimide-*S*-glutathione (GS-NEM) [26–31]. Third, NEM inhibits glutathione reductase, blocking the reduction of GSSG to GSH [18]. Finally, NEM requires only a short incubation time. Despite these advantages, however, NEM is not suitable for use in spectrophotometric methods due to enzyme inhibition [16,17].

Here, we studied the relationship between UPE and intracellular GSH/GSSG ratio as an indicator of oxidative stress marker in differentiated HL-60 cells. The respiratory burst was induced in HL-60 cells using phorbol 12-myristate 13-acetate (PMA), and UPE intensity was measured for 9000 s [7,14]. The intracellular levels of glutathione (GS-NEM and GSSG) were measured in cell pellets collected during this time interval and analyzed using CE-MS. Finally, the GS-NEM/GSSG ratio was calculated, and the relationship between the dynamic UPE profile and glutathione levels was determined.

2. Methods

2.1. Culture, Differentiation, and Induction of Respiratory Burst in HL-60 Cells

HL-60 cells (CCL-240; American Type Culture Collection, ATCC, Manassas, VA) were cultured in Iscove's Modified Dulbecco's Medium (IMDM) without phenol red (Gibco-Life Technologies, Grand Island, NY) supplemented with 10% (v/v) fetal calf serum and 1% (v/v) penicillin/streptomycin (Sigma-Aldrich, St. Louis, MO). Cells were seeded at 0.2×10^6 cells/ml and maintained in the exponential growth phase in a CO_2 incubator at 37 °C in accordance with the instructions provided by ATCC. The trypan-blue exclusion method was used to count the cells and determine their viability (> 85%) with an automated cell counter (Bio-Rad, Hercules, CA).

During a new cell passage, the cells were split into two flasks. The cells in one flask were differentiated by the addition of freshly prepared 1 μM all-*trans*-retinoic acid (ATRA; Sigma-Aldrich) in DMSO (differentiated cells); the cells in the other flask received no treatment (undifferentiated control cells). The cells were then incubated for up to 7 days. PMA (54 nM, Sigma-Aldrich) was then applied in order to induce respiratory burst, and UPE was measured. All experiments were performed on cells at passage number P10 or P11.

2.2. Experimental Design

In this study, we used an optimized experimental design (see Supplementary Fig. 1) based on our previous studies [7,14]. On day 7, PMA was applied to the differentiated and control cells in order to induce respiratory burst. At four times points (TP1, TP2, TP3, and TP4), cell samples were collected and used to measure GSH and GSSG. Aliquots of 10^7 cells per time point were used for the colorimetric assay and CE-MS analysis. UPE was measured for 9000 s (2.5 h) after PMA induction. TP1 corresponds to the samples which were collected and analyzed before PMA induction; TP2 samples after 60 s, TP3 after 4500 s and TP4 after 9000 s respectively.

2.3. Ultra-weak Photon Emission

A series 9558B photomultiplier tube equipped with an S20 photocathode (ET Enterprises, Sweetwater, TX) was used to record the UPE profile. The detector was cooled to − 25 °C in order to reduce noise. Photon emission intensity (in counts/second) was recorded for 9000 s in a dark chamber that was maintained at 37 °C using a Peltier element. To measure UPE, a 6-ml aliquot of suspended cells was transferred to the dark chamber immediately after induction with PMA (54 nM).

2.4. Sample Collection and Quenching of the Cell Pellets

For GS-NEM and GSSG analysis, 10^7 cells were collected at specific time points (see Supplementary Fig. 1), centrifuged for 4 min at 1000 rpm, and the supernatant (culture medium) was discarded. The cell pellets were resuspended in 1 ml cold (0–2 °C) saline solution containing 0.9% NaCl and 1.5 mg/ml ethylenediaminetetraacetic acid (EDTA; Merck, Darmstadt, Germany). To analyze GSH and GSSG using our CE-MS approach, 50 mM NEM (Sigma-Aldrich) was added to the saline solution. The cells were centrifuged for 4 min at 1000 rpm, the supernatant was discarded, and the cell pellets were stored at − 80 °C until analysis.

2.5. CE-MS

2.5.1. Sample Preparation

To extract the adduct GS-NEM and GSSG, the cell pellets were resuspended in 250 µl ice cold (− 20 °C) MeOH (80%; Biosolve BV, Valkenswaard, the Netherlands) containing 5 mM NEM. The samples were processed in a bullet blender for 2 min on setting 8. The lysed cell suspension was then transferred to a 0.5-ml Eppendorf tube and dried in a speed-vac. The dried samples were resuspended in 20 µl of 250 mM ammonium acetate (Sigma-Aldrich), vortexed for 5 min at speed 8, centrifuged for 5 min at 13.2 rpm, and transferred to vials for CE-MS analysis.

2.5.2. CE-MS Methodology

CE-MS was performed using an Agilent CE 7100 system (Agilent Technologies, Palo Alto, CA) coupled to an Agilent 6230 time-of-flight mass spectrometer. CE was coupled to MS via a sheath-liquid interface using an Agilent 1100 isocratic HPLC pump. The sheath-liquid was a mixture of water, methanol, and formic acid (50/50/0.1, v/v/v) that was delivered at a flow rate of 10 µl/min. An Agilent G1603A adapter kit and an Agilent G1607A CE-ESI-MS sprayer kit (Agilent Technologies, Waldbronn, Germany) were used for the linking, and an Agilent Mass Hunter Workstation was used to control the system and to acquire the data.

For the separation, a 90-cm long, bare fused-silica capillary (ID: 50 µm; Polymicro Technologies, Palo Alto, CA) was used, with 1 M formic acid (pH 1.8; Acros Organics, Geel, Belgium) as the background electrolyte (BGE). Milli-Q water (EMD Millipore, Billerica, MA) and 1 M NaOH (Merck) were used for capillary pre-conditioning. Prior to each run, the capillary was preconditioned by rinsing sequentially with water, sodium hydroxide, water, and BGE for 2 min at the pressure of 935 mbar.

Samples were injected hydrodynamically by applying a pressure of 50 millibars for 120 s, corresponding to circa 120 nl; this relatively high volume of sample injection was possible due to the application of dynamic pH junction [32]. After sample injection, a plug of BGE was added at a pressure of 50 millibars for 10 s. Voltage (30 kV) was then applied for 30 min at 25 °C. Electrospray ionization-mass spectrometry (ESI-MS) was performed in the positive-ion mode. The capillary, fragmentor, and skimmer voltages were set to 4000, 100, and 50 V, respectively. The nebulizer pressure was 5 psi, and the drying gas was delivered at 7 l/min at 300 °C. Data were recorded at a rate of 1.5 cycles per second (range: 50–1000 m/z). GS-NEM and GSSG were identified according to accurate mass and migration time using standard compounds as a reference. Standard solutions of GS-NEM (prepared in-house using a mixture of glutathione obtained from Cayman Chemicals and NEM) and GSSG (Sigma-Aldrich) were prepared fresh in Milli-Q water. The peak areas obtained for GS-NEM and GSSG were corrected using an internal standard (response ratio) and were then used to calculate the GSH/GSSG ratio.

2.6. Spectrophotometric Assay

Total GSH (GSH + GSSG) and oxidized glutathione (GSSG) were measured using a spectrophotometric assay (enzymatic recycling method; Sigma-Aldrich). The samples were prepared and measured at room temperature in accordance with the protocol provided the manufacturer. In brief, pellets containing 10^7 cells per time point were lysed, the proteins were precipitated, and the samples were centrifuged. The supernatant was then split into two aliquots. One aliquot (10 µl) was diluted 50 × and used to measure total GSH; the other aliquot (120 µl) was used undiluted to measure GSSG. GSH concentration was calculated using the following equation: GSH = total glutathione (GSH + GSSG) – GSSG × 2.

2.7. Statistical Analysis

GraphPad Prism version 7.0 was used to create the smoothed UPE curve. We smoothed the curve using the function xy analysis (smooth - 2nd order of smoothing with 100 neighbors data points). Next, the smoothed data were normalized by the highest UPE intensity. The results obtained for levels of GS-NEM, GSSG and GS-NEM/GSSG ratio were uploaded to the web-based tool MetaboAnalyst for statistical analysis [33–35]. Data were log-transformed and auto-scaled in order to obtain a normal distribution [36]. Changes in GS-NEM and GSSG were analyzed over the four-time points using an ANOVA. The correlation between the UPE data and GSH levels was analyzed using Spearman's correlation coefficient (SPSS version 23; IBM Corp., Armonk, NY).

3. Results

3.1. Ultra-weak Photon Emission

First, we differentiated HL-60 cells into neutrophil-like cells by incubating the cells in ATRA for 7 days. We then stimulated both differentiated and undifferentiated (control-treated) cells with PMA in order to induce respiratory burst. The UPE profile was then measured for 9000 s after PMA stimulation, as shown in Fig. 2.

Differentiated cells had a stronger PMA-induced UPE response compared to undifferentiated cells, consistent with the production of higher amounts of ROS [7,14]. Therefore, we hypothesized that intracellular glutathione (GSH) levels decrease during respiratory burst due to increased levels of ROS, thereby leading to oxidative stress conditions.

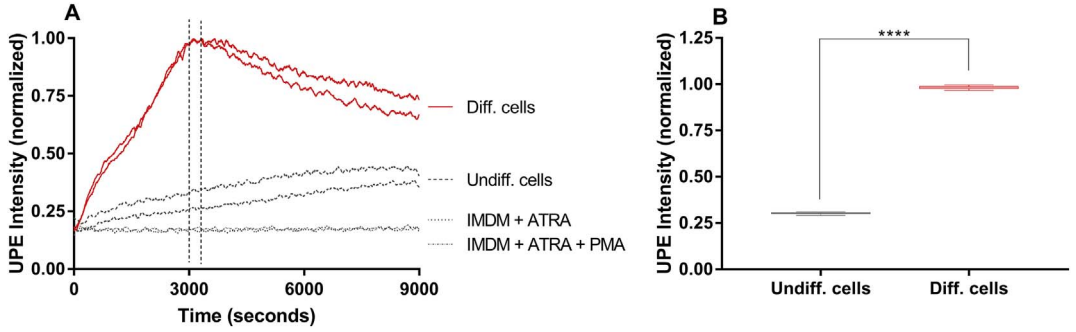

Fig. 2. UPE profiles measured in differentiated and undifferentiated HL-60 cells during respiratory burst. (A) Cell suspensions (10^6 cells/ml) were recorded in the dark at 37 °C for 9000 s following PMA stimulation. The lines (duplicate measurements) represent the normalized smoothed curve of 100 points. Control experiments were performed with medium IMDM + ATRA and medium IMDM + ATRA + PMA (B) Interval Analysis (analysis between 3000 and 3600 s as indicated in A). Student's paired *t*-test performed with ****$p < 0.0001$.

3.2. Intracellular GS-NEM and GSSG Levels Measured Using CE-MS

Next, we examined the relationship between glutathione levels (GSH and GSSG) and the UPE profile using CE-MS to measure the levels of GSH and GSSG. We used the alkylating agent NEM when collecting the cell samples, allowing us to measure the adduct GS-NEM. We measured the intracellular levels of GS-NEM and GSSG in PMA-stimulated differentiated and undifferentiated HL-60 cells and compared the results with the dynamic UPE profile. Cells were collected and analyzed at four time points relative to PMA stimulation (see Fig. S1).

Fig. 3 shows GS-NEM and GSSG levels measured using CE-MS. The levels of GS-NEM were similar between undifferentiated and differentiated cells, peaking at the second time point (TP2); in contrast, GSSG levels differed significantly, with a steep increase in the differentiated cells at TP3 and TP4. Thus, the GS-NEM/GSSG ratio — which is commonly used as a marker for cellular redox state — was significantly lower in the differentiated cells at TP3 and TP4. Intragroup ANOVA analysis revealed significant changes in the concentrations of GS-NEM, GSSG, and the GS-NEM/GSSG ratio in the differentiated cells over the four time points (see Fig. 3 and Table S1).

3.3. Correlation Between UPE and Glutathione Levels

Table 1 shows the Spearman's rank results obtained for the correlation between UPE data and the GS-NEM, GSSG and GS-NEM/GSSG ratio. Interestingly, there is an absence of significant correlations (*p*-values > 0.05) although it shows correlation coefficients (r_s) ≥ 0.6.

Table 1
Spearman's rank correlation between the UPE and glutathione levels.

Compound	Cell type	Correlation coefficient (r_s)	*p*-Value
GS-NEM	Diff. cells	− 0.6	0.4
	Undiff. cells	− 0.6	0.4
GSSG	Diff. cells	0.8	0.2
	Undiff. cells	0.0	1.0
GS-NEM/GSSG	Diff. cells	− 0.8	0.2
	Undiff. cells	− 0.8	0.2

4. Discussion

Treating HL-60 cells with ATRA causes the cells to differentiate into neutrophil-like cells [37]. During the respiratory burst, neutrophils are responsible for the first line of defense by generating high amounts of reactive oxygen species (ROS) in order to kill invading pathogens [38]. Because UPE is correlated with ROS production, it is considered a viable tool for monitoring dynamic oxidative processes in biological systems [7]. Glutathione is an endogenous cellular antioxidant that modulates physiological levels of ROS and is involved in the cell's response to oxidative stress [11]. Our goal was to study the role of glutathione in differentiated HL-60 cells during respiratory burst [7,14] and compare the UPE profile with glutathione (GS-NEM and GSSG) measured using our optimized CE-MS approach.

Several groups reviewed the challenges and pitfalls associated with analyzing glutathione in biological samples [18,19,25]. Sample preparation is a critical step in the process, as GSH can undergo enzymatic and non-enzymatic autoxidation catalyzed by γ-glutamyltranspeptidase. GSH can also interact with and bind to proteins via S—H bonds, leading to the removal of GSH during sample preparation. Therefore, it is important to protect the thiol group during sample preparation in order to avoid possible miscalculations. Compared with spectrophotometric methods for measuring GSH, chromatographic methods have many advantages, including high specificity and the ability to detect concentrations in the picomolar range [39]. CE is in particular suited for the highly efficient analysis of polar and charged metabolites as compounds are separated according to their charge-to-size ratio. CE in combination with TOF-MS has proven to be a very efficient and selective tool for the separation of charged metabolites in

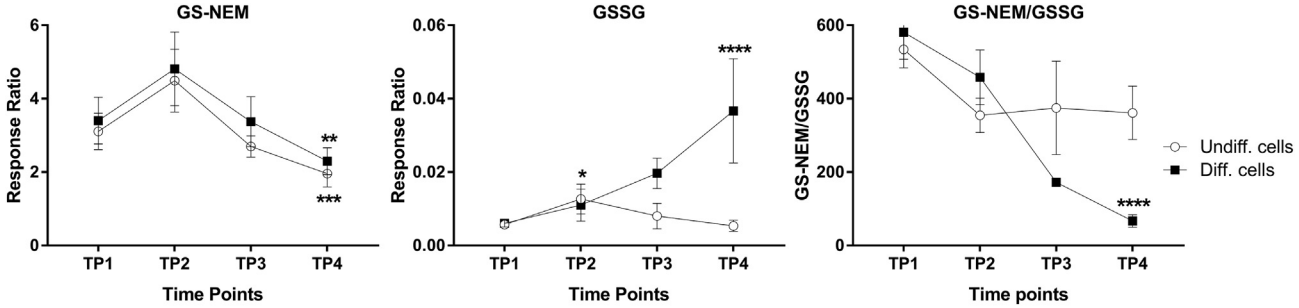

Fig. 3. Intracellular levels of GS-NEM, GSSG, and GS-NEM/GSSG ratio measured in differentiated and undifferentiated HL-60 cells during PMA induced respiratory burst. GS-NEM and GSSG levels were measured using CE-MS. Intragroup ANOVA was performed over the four time points to analyze the differences in glutathione levels. Data are plotted as the mean (n = 3) ± SD. *$p < 0.05$, **$p < 0.01$, ***$p < 0.001$, and ****$p < 0.0001$. TP1, TP2, TP3, and TP4 correspond to 0, 60, 4500, and 9000 s, respectively, relative to PMA stimulation.

biological samples [40,41]. Additional advantages of CE-MS include the capability to deal with biomass-limited samples and low solvent consumption [40,41].

Our optimized CE-MS method clearly demonstrates that GSH is readily oxidized during sample preparation, as samples collected and analyzed in the absence of the alkylating agent NEM contain GSSG, reflecting the auto-oxidation of GSH during sample manipulation (see Figs. S2 and S3). Therefore, it is important to use an alkylating agent such as NEM in order to prevent the auto-oxidation of GSH, thereby increasing the accuracy of the GSH/GSSG ratio.

Our GS-NEM and GSSG measurements using CE-MS show that glutathione levels (GS-NEM and GSSG) change in differentiated cells during respiratory burst, leading to cellular oxidative damage (i.e., a decrease in the GS-NEM/GSSG ratio). To support our results obtained using CE-MS, we also measured glutathione levels (total GSH and GSSG) using the conventional enzymatic recycling assay (see Fig. S4), and we measured total GSH using our validated LC-MS platform [42] (see Fig. S5). The results obtained using these additional analyses are consistent with our CE-MS results. Although it is not possible to compare the absolute concentrations obtained in the spectrophotometric assay with the results obtained using CE-MS or LC-MS, we found a similar trend with respect to total GSH, GSSG, and the calculated cellular redox ratio (GSH/GSSG). However, the absolute concentrations of total GSH in our study were in the micromolar range, and the GSH/GSSG ratio was considerably lower than the ratio obtained using our CE-MS approach, as well as previously reported values [19,43].

Here, we attempted to determine the association between UPE and the GSH/GSSG ratio in HL-60 cells during respiratory burst. In differentiated cells, glutathione (GS-NEM and total GSH) levels were significantly decreased, whereas the levels of GSSG increased significantly, causing a decrease in the GS-NEM/GSSG ratio and leading to cellular oxidation conditions. However, we found no statistically significant correlation between the UPE profile and glutathione levels. In neutrophils, intracellular GSH levels decrease during respiratory burst, whereas glutathione synthesis and glutathione recycling pathways are upregulated in order to maintain homeostasis [44,45]. Because glutathione is an endogenous antioxidant, its response is relatively rapid; in contrast, the UPE profile likely reflects the sum of all oxidative processes. Thus, additional pathways are probably involved, operating at several organizational levels on a variety of time scales, possibly explaining the apparent lack of significant correlation between the GSH/GSSG ratio and the UPE profile. In addition to that, the respiratory burst is a physiological mechanism of defense capable to restore homeostasis.

Severe oxidative stress is the uncontrolled ROS formation overpowering the inherent homeostasis-restoring ability and consequently, it affects the process of GSSG being reduced to GSH, causing the accumulation of GSSG in cells [46]. Another hypothesis to be considered is that under such prolonged oxidative conditions GSSG can be eventually exported out of the cells to prevent a cellular shift in the redox equilibrium [47]. Therefore, prolonged exposed time of cellular oxidative conditions is required for the observation of glutathione depletion. In conclusion, there are many other biochemical processes which might be taken into consideration and that probably explain the absence of direct and significant correlation.

5. Conclusions and Future Perspectives

In summary, we have used our optimized CE-MS approach as a tool for measuring the GSH/GSSG ratio in cellular extracts. Intracellular GSH/GSSG ratio was measured during the oxidative burst, and the results were compared with dynamic UPE data recorded over the same time period. Although the GSH/GSSG ratio decreased in differentiated cells during respiratory burst, we found no statistically significant correlation between GSH/GSSG ratio and the UPE profile.

This experimental design can be expanded in future studies in order to increase the time exposure of cellular oxidative conditions, including more time points. In addition, computational models may provide mechanistic insight into the chemical kinetics processes that underlie UPE, thereby providing predictive value and the ability to better interpret UPE data.

Acknowledgments

This work was supported by CNPq (230827/2012-8) (the National Council for Scientific and Technological Development, Brazil). RCRB is the recipient of a scholarship from Science without Borders (scholarship number 230827/2012-8). The authors thank Johannes Cornelius Schoeman for valuable and constructive suggestions regarding the biochemistry experiments and Prof. Ruud Berger for the discussions and revision of the biochemical content described in this research.

Appendix A. Supplementary Data

Supplementary data to this article can be found online at http://dx.doi.org/10.1016/j.jphotobiol.2017.09.002.

References

[1] M. Cifra, P. Pospisil, Ultra-weak photon emission from biological samples: definition, mechanisms, properties, detection and applications, J. Photochem. Photobiol. B 139 (2014) 2–10.
[2] P. Pospisil, A. Prasad, M. Rac, Role of reactive oxygen species in ultra-weak photon emission in biological systems, J. Photochem. Photobiol. B 139 (2014) 11–23.
[3] T. Finkel, N.J. Holbrook, Oxidants, oxidative stress and the biology of ageing, Nature 408 (6809) (2000) 239–247.
[4] T. Heitzer, et al., Endothelial dysfunction, oxidative stress, and risk of cardiovascular events in patients with coronary artery disease, Circulation 104 (22) (2001) 2673–2678.
[5] M.T. Lin, M.F. Beal, Mitochondrial dysfunction and oxidative stress in neurodegenerative diseases, Nature 443 (7113) (2006) 787–795.
[6] W.R. Markesbery, Oxidative stress hypothesis in Alzheimer's disease, Free Radic. Biol. Med. 23 (1) (1997) 134–147.
[7] R.C.R. Burgos, et al., Ultra-weak photon emission as a dynamic tool for monitoring oxidative stress metabolism, Sci Rep 7 (1) (2017) 1229.
[8] S. Birtic, et al., Using spontaneous photon emission to image lipid oxidation patterns in plant tissues, Plant J. 67 (6) (2011) 1103–1115.
[9] A. Prasad, P. Pospisil, Linoleic acid-induced ultra-weak photon emission from *Chlamydomonas reinhardtii* as a tool for monitoring of lipid peroxidation in the cell membranes, PLoS One 6 (7) (2011) e22345.
[10] A. Meister, M.E. Anderson, Glutathione, Annu. Rev. Biochem. 52 (1) (1983) 711–760.
[11] G. Wu, et al., Glutathione metabolism and its implications for health, J. Nutr. 134 (3) (2004) 489–492.
[12] S.C. Lu, Glutathione synthesis, Biochim. Biophys. Acta 1830 (5) (2013) 3143–3153.
[13] M. Asensi, et al., Ratio of reduced to oxidized glutathione as indicator of oxidative stress status and DNA damage, Methods in Enzymology, Academic Press, 1999, pp. 267–276.
[14] R.C.R. Burgos, et al., Tracking biochemical changes correlated with ultra-weak photon emission using metabolomics, Journal of Photochemistry and Photobiology B-Biology 163 (2016) 237–245.
[15] R. Brigelius, et al., Identification and quantitation of glutathione in hepatic protein mixed disulfides and its relationship to glutathione disulfide, Biochem. Pharmacol. 32 (17) (1983) 2529–2534.
[16] I. Rahman, A. Kode, S.K. Biswas, Assay for quantitative determination of glutathione and glutathione disulfide levels using enzymatic recycling method, Nat. Protoc. 1 (6) (2006) 3159–3165.
[17] F. Tietze, Enzymic method for quantitative determination of nanogram amounts of total and oxidized glutathione: applications to mammalian blood and other tissues, Anal. Biochem. 27 (3) (1969) 502–522.
[18] E. Blonska-Sikora, et al., Glutathione: method of sample preparation for chromatography and capillary electrophoresis, Chem. Aust. 66 (2012) 929–942.
[19] D. Giustarini, et al., Pitfalls in the analysis of the physiological antioxidant glutathione (GSH) and its disulfide (GSSG) in biological samples: an elephant in the room, J. Chromatogr. B Anal. Technol. Biomed. Life Sci. 1019 (2016) 21–28.
[20] Y. Iwasaki, et al., Chromatographic and mass spectrometric analysis of glutathione in biological samples, J. Chromatogr. B Anal. Technol. Biomed. Life Sci. 877 (28) (2009) 3309–3317.
[21] E. Camera, M. Picardo, Analytical methods to investigate glutathione and related compounds in biological and pathological processes, J. Chromatogr. B Anal. Technol. Biomed. Life Sci. 781 (1–2) (2002) 181–206.
[22] L.A. D'Agostino, et al., Comprehensive plasma thiol redox status determination for metabolomics, J. Proteome Res. 10 (2) (2011) 592–603.
[23] R. Lee, P. Britz-McKibbin, Differential rates of glutathione oxidation for assessment of cellular redox status and antioxidant capacity by capillary electrophoresis-mass

spectrometry: an elusive biomarker of oxidative stress, Anal. Chem. 81 (16) (2009) 7047–7056.
[24] O.W. Griffith, Determination of glutathione and glutathione disulfide using glutathione-reductase and 2-vinylpyridine, Anal. Biochem. 106 (1) (1980) 207–212.
[25] P. Monostori, et al., Determination of glutathione and glutathione disulfide in biological samples: an in-depth review, J. Chromatogr. B Anal. Technol. Biomed. Life Sci. 877 (28) (2009) 3331–3346.
[26] D. McLaggan, et al., Glutathione-dependent conversion of *N*-ethylmaleimide to the maleamic acid by *Escherichia coli*: an intracellular detoxification process, Appl. Environ. Microbiol. 66 (4) (2000) 1393–1399.
[27] E.R. Mojica, S. Kim, D.S. Aga, Formation of *N*-ethylmaleimide (NEM)-glutathione conjugate and *N*-ethylmaleamic acid revealed by mass spectral characterization of intracellular and extracellular microbial metabolites of NEM, Appl. Environ. Microbiol. 74 (1) (2008) 323–326.
[28] D.G. Smyth, O.O. Blumenfeld, W. Konigsberg, Reactions of *N*-ethylmaleimide with peptides and amino acids, Biochem. J. 91 (3) (1964) 589–595.
[29] G. Gorin, P. Martic, G. Doughty, Kinetics of the reaction of *N*-ethylmaleimide with cysteine and some congeners, Arch. Biochem. Biophys. 115 (3) (1966) 593–597.
[30] N. Haugaard, J. Cutler, M.R. Ruggieri, Use of *N*-ethylmaleimide to prevent interference by sulfhydryl-reagents with the glucose-oxidase assay for glucose, Anal. Biochem. 116 (2) (1981) 341–343.
[31] J.R. Heitz, C.D. Anderson, B.M. Anderson, Inactivation of yeast alcohol dehydrogenase by N-alkylmaleimides, Arch. Biochem. Biophys. 127 (1) (1968) 627–636.
[32] Y.H. Tak, G.W. Somsen, G.J. de Jong, Optimization of dynamic pH junction for the sensitive determination of amino acids in urine by capillary electrophoresis, Anal. Bioanal. Chem. 401 (10) (2011) 3275–3281.
[33] J. Xia, et al., MetaboAnalyst 2.0—a comprehensive server for metabolomic data analysis, Nucleic Acids Res. 40 (Web Server issue) (2012) W127–33.
[34] J. Xia, et al., MetaboAnalyst: a web server for metabolomic data analysis and interpretation, Nucleic Acids Res. 37 (Web Server issue) (2009) W652–60.
[35] J. Xia, et al., MetaboAnalyst 3.0—making metabolomics more meaningful, Nucleic Acids Res. 43 (W1) (2015) W251–7.
[36] R.A. van den Berg, et al., Centering, scaling, and transformations: improving the biological information content of metabolomics data, BMC Genomics 7 (1) (2006) 142.
[37] T.R. Breitman, S.E. Selonick, S.J. Collins, Induction of differentiation of the human promyelocytic leukemia cell line (HL-60) by retinoic acid, Proc. Natl. Acad. Sci. U. S. A. 77 (5) (1980) 2936–2940.
[38] C. Dahlgren, A. Karlsson, Respiratory burst in human neutrophils, J. Immunol. Methods 232 (1–2) (1999) 3–14.
[39] K. Dettmer, P.A. Aronov, B.D. Hammock, Mass spectrometry-based metabolomics, Mass Spectrom. Rev. 26 (1) (2007) 51–78.
[40] A. Hirayama, T. Soga, CE-MS in metabolomics, Capillary Electrophoresis–Mass Spectrometry (CE-MS), Wiley-VCH Verlag GmbH & Co. KGaA, 2016, pp. 293–314.
[41] P. Britz-McKibbin, Capillary electrophoresis–electrospray ionization-mass spectrometry (CE–ESI-MS)-based metabolomics, in: T.O. Metz (Ed.), Metabolic Profiling: Methods and Protocols, Humana Press, Totowa, NJ, 2011, pp. 229–246.
[42] M.J. Noga, et al., Metabolomics of cerebrospinal fluid reveals changes in the central nervous system metabolism in a rat model of multiple sclerosis, Metabolomics 8 (2) (2012) 253–263.
[43] O. Zitka, et al., Redox status expressed as GSH:GSSG ratio as a marker for oxidative stress in paediatric tumour patients, Oncol. Lett. 4 (6) (2012) 1247–1253.
[44] M. Bilzer, B.H. Lauterburg, Glutathione metabolism in activated human neutrophils: stimulation of glutathione synthesis and consumption of glutathione by reactive oxygen species, Eur. J. Clin. Investig. 21 (3) (1991) 316–322.
[45] A.A. Voetman, J.A. Loos, D. Roos, Changes in the levels of glutathione in phagocytosing human neutrophils, Blood 55 (5) (1980) 741–747.
[46] S.C. Lu, Regulation of glutathione synthesis, Mol. Asp. Med. 30 (1–2) (2009) 42–59.
[47] S.C. Lu, Regulation of hepatic glutathione synthesis: current concepts and controversies, FASEB J. 13 (10) (1999) 1169–1183.